Adaptive Power Oscillation Damping Control via VSC-HVDC for the Great Britain Power Grid

Yuqing Dong[1], Yi Zhao[1], Khaled Alshuaibi[1], Chengwen Zhang[1], Yilu Liu[1,2]
1. *The University of Tennessee*
Knoxville, TN, USA
2. *Oak Ridge National Laboratory*
Oak Ridge, TN, USA
{ydong22, liu}@utk.edu

Lin Zhu[3], Evangelos Farantatos[3]
3. *Electric Power Research Institute (EPRI)*
Palo Alto, CA, USA
{lzhu, efarantatos}@epri.com
Kaiqi Sun[4]
4. *Shandong University*
Jinan, Shandong, China
skq@sdu.edu.cn

Benjamin Marshall[5], Md Rahman[5], Oluwole Adeuyi[5], Simon Marshall[5], Ian L. Cowan[5]
5. *The National HVDC Centre*
UK
{Benjamin.Marshall, Md.Rahman, Oluwole.Adeuyi, simon.marshall Ian.L.Cowan2}@sse.com

***Abstract*—With the frequent and uncertain variations of loads and renewable generation in the power system, a conventional power oscillation damping (POD) controller with fixed parameters cannot guarantee satisfactory control performance when power system operating conditions change. In this paper, an adaptive wide-area POD is proposed via voltage source converter based high voltage direct current (VSC-HVDC) system to achieve sufficient control effect under different system dispatches. The observation signal and actuator for the POD can be selected in advance considering the system dispatches. Meanwhile, the POD parameters can be adjusted online based on a measurement-driven approach. Simulations of the Great Britain power grid model on the real time digital simulator (RTDS) demonstrate that the adaptive POD can improve the control performance compared to a conventional non-adaptive POD.**

Keywords—adaptive control, power oscillation damping, RTDS, VSC-HVDC

I. INTRODUCTION

In today's interconnected power grids, low-frequency oscillations are a significant issue that can limit power transfer capability and even deteriorate power system security due to potential low damped or even undamped oscillations [1]-[3].

With the increasing integration of renewables and the retirement of conventional synchronous generators, the stability properties of the system and, in particular, the oscillation modes (e.g., oscillation frequency, damping ratio, and mode shape) may change due to the different dynamics of the control of inverter-based resources and their tracking of the network compared to synchronous machines [4]-[5]. Moreover, new oscillation modes could emerge as a result of this generation mix evolution [6]-[7].

Typically, local controllers (e.g., power system stabilizers on synchronous generators) have been used to suppress these low-frequency oscillations [8]. However, the retirement of conventional plants will result in insufficient stabilizing capability from the remaining generators, the location of which may also render them inappropriate to suppress these oscillations [9]. The use of inverter-based resources, Flexible AC Transmission Systems (FACTS) devices, and high voltage direct current (HVDC) links with appropriate controls to provide damping is envisioned as a solution to this challenge. Due to the power electronics interface with the grid, these devices can provide fast and flexible control that can outperform slower control provided by generators [10]-[11].

Another challenge introduced by high levels of renewables is the frequent and uncertain variations in the operating conditions of the grid [12]. This may result in frequently varying oscillation modes that are dependent on the operating condition [13]. In conventional power grids with limited variability and uncertainty, the oscillation damping controllers are designed based on the system circuit model around a particular operating point and tuned for hypothetical critical operating conditions [14]. Such controllers with fixed parameters may experience deterioration in the damping performance when the system operation condition varies. To address these challenges, the adaptive capability should be considered in the design of the damping controller [15]. Some papers have investigated adaptive damping controllers in different application areas. Reference [16] develops a damping controller via Thyristor Controlled Series Compensator (TCSC) to suppress inter-area power oscillations based on the proposed oscillation energy analysis. Reference [17] proposes a linearized Heffron-Philips model and designs an adaptive neuro-fuzzy UPFC controller to provide efficient damping control. In [18], a single-input single-output adaptive damping control is proposed on the FACTS devices to provide system damping control.

As synchronized measurements provided by phasor measurement units (PMUs) are increasingly available in transmission networks, the design and development of such adaptive wide-area PODs become feasible and an urgent need [19]-[20]. To this end, a simple linear transfer function model can be built using the collected measurements to reflect operating condition variations. The PODs can automatically select the effective observation signal(s) as the controller input

This work was primarily supported by The National HVDC Centre and Electric Power Research Institute (EPRI), and partly supported by National Science Foundation under the Award Number 1839684 and 1941101. This work also made use of Engineering Research Center Shared Facilities supported by the Engineering Research Center Program of the National Science Foundation and DOE under NSF Award Number EEC-1041877 and the CURENT Industry Partnership Program.

signal(s), select the effective actuator(s), and adjust their parameters based on the identified measurement-driven models to achieve the desired damping performance.

In this paper, an adaptive wide-area POD controller through voltage source converter based HVDC (VSC-HVDC) links based on a measurement-driven approach is proposed for the Great Britain (GB) power grid. The proposed POD controller has the following features:

1) The designed POD controller can suppress the targeted oscillation mode by modulating the active power and/or reactive power of the selected VSC-HVDC link.

2) Under different system dispatches, the designed POD controller can switch its input/feedback signal and actuator using a loop-up table.

3) When the GB power grid is operating under different system dispatches, the POD controller can adjust its control parameters using the measurement-driven approach to guarantee its control performance.

The rest of this paper is organized as follows. Section II presents an overview of the GB grid model. Section III introduces the POD design method, including the selection of effective signal and actuator. Case studies conducted on RTDS are presented in Section IV. Section V draws the final conclusions.

II. Introduction of GB Model

In this paper, a reduced 36-bus model implemented in DigSILENT/PowerFactory and developed by National Grid Electricity System Operator (National Grid ESO), is used to represent the GB power system. The system topology is shown in Figure 1, with 13 international HVDC links and five domestic HVDC links.

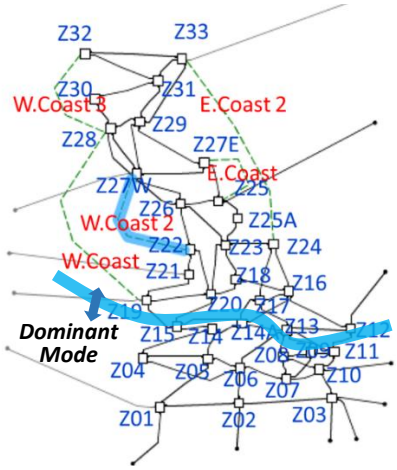

Figure 1. Diagram of Great Britain power system.

Among the five domestic HVDC links, the W.Coast HVDC is an LCC-HVDC link, while the other four (W.Coast HVDC 2, W.Coast HVDC 3, E.Coast, and E.Coast 2) are VSC-HVDC links. Each bus has eight synchronous generators based on different fuels (biomass, coal, gas, nuclear, hydro, pump storage, oil, and other), one wind plant, one solar plant, and one aggregated load. All synchronous generators are equipped with a governor, exciter, and automatic voltage regulator. The synchronous generators with the fuel type of biomass, nuclear, gas, hydro, and pump storage are equipped with local PSSs. All the renewables and HVDC links are represented by static generators. They are equipped with user-defined active power controllers and voltage controllers to modulate active power output and maintain the local voltage, respectively.

Modal analysis is first conducted based on the GB model. Under the default dispatch with intermediate load, the dominant mode with low damping can be observed and marked in Figure 1. This mode is the oscillation between the generators in the northern vs. southern GB. This oscillation mode is selected as the target mode, which needs to be suppressed by the POD controller.

III. Adaptive POD Design Method

A. Adaptive POD Design method overview

The adaptive POD design method is shown in Figure 2. The adaptive capabilities of the POD is conducted from two aspects:

1) Optimal observasion signal and actuator, i.e., control loop selection, for different system operating condition, which will be introduced in Section III. B.

2) The POD parameters are calculated according to the measurement-driven approach in Section III. C. This is the core adaptive part that can achieve online updates.

B. Observation Signal and Actuator Selection Method

With the increasing installations of PMUs, a great number of candidate observation signals collected by PMUs can be utilized for oscillation mode analysis and control. However, since only some of them have good observability of the dominant oscillation mode, a comprehensive method is needed to select the effective observation signal for the critical mode among all the candidate observation signals under different operating conditions.

In this work, a series of three-phase fault events at different locations are used to excite the oscillation mode of interest. The Fast Fourier Transform (FFT) algorithm is adopted to select the optimal observation signals of the damping control loop by utilizing the simulation output signals collected from the fault events. For each case, the signals are ranked from high to low according to the magnitudes at the frequency of the targeted oscillation mode. The highest-ranking signal is selected as the observation signal to suppress this dominant mode.

Since different HVDCs have different controllability to the system oscillation modes, the residue method is utilized to analyze the sensitivity of all candidate actuation signals to the observation signal and to select the optimal actuator. The transfer function $G(s)$ is obtained from the input u_i to the output y_j, and it can always be expressed as a sum of partial fractions of the form:

$$G(s) = \sum_{k=1}^{n} \frac{R_k}{s - \lambda_k} \tag{1}$$

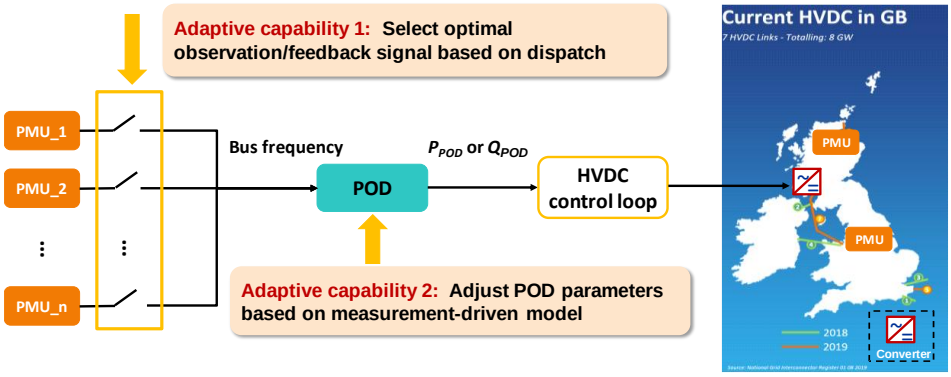

Figure 2. Adaptive POD design.

where R_k is the residue associated with the mode λ_k. The residue R_k provides an idea of how the mode λ_k is affected by the input u_i and how visible it is from the output y_j. The optimal input-output signal pair is given by the maximum value of the residue magnitude.

C. *POD parameter calculation based on measurement-driven approach*

The measurement-driven approach is used to design the POD controller. The POD controller uses the selected effective observation PMU measurement as the input signals, and its control command is added to P_{ref} and/or Q_{ref} to suppress the targeted oscillation mode by modulating the active power or reactive power of the selected HVDC link. In this paper, the auxiliary POD control via VSC-HVDC links is investigated to damp the low-frequency oscillation. To get the realistic dynamic oscillation properties of the entire system for POD design, a probing signal is added to P_{ref} and Q_{ref}, and the corresponding feedback signal response is collected for constructing the measurement-driven model with the prediction error method (PEM) [21].

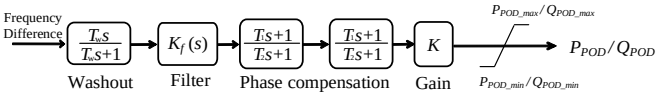

Figure 3. POD structure.

Figure 3 illustrates the block diagram of the POD controller, which consists of a washout block, a band-pass filter, two phase compensation blocks, and a gain block [22]. The input signal of the POD is selected based on FFT analysis result, and the controller parameters are designed based on the identified measurement-based model. The output signal of POD P_{POD}/Q_{POD} is added as an auxiliary signal to the P_{ref} to modulate the active power, or to the Q_{ref} to modulate the reactive power of the HVDC links.

The time constant T_w of the washout block is set as 10s. The transfer function $K_f(s)$ of the filter is [23]:

$$K_f(s)=\frac{\frac{\omega_n}{Q}s}{s^2+\frac{\omega_n}{Q}s+\omega_n^2} \tag{2}$$

where ω_n is the oscillation frequency of the targeted mode. Q is the quality factor, which is usually set to be 1.

In the phase compensation block, T_1 and T_2 are the lead and lag time constant, respectively. K is the gain of the POD. P_{POD_max}/Q_{POD_max} and P_{POD_min}/Q_{POD_min} are the upper and lower limits of the POD output.

According to R_k associated with the inter-area oscillation mode λ_k, the compensation angle of POD satisfies

$$\angle K(j\omega_d)+\angle R_k=-180^\circ \tag{3}$$

and the amplitude satisfies

$$\left|K(j\omega_d)\right|\cdot\left|R_k\right|=\left|-(\varsigma_*-\varsigma_k)\omega_d\right| \tag{4}$$

where ω_d and ς_k are the frequency and damping ratio of the dominant inter-area oscillation mode. ς_* is the expected damping ratio.

The parameters of $K(s)$ can be calculated with the following equations [24]:

$$\begin{cases}\alpha=(1+\sin\theta_{\max})/(1-\sin\theta_{\max}),\theta_{\max}=\angle K(j\omega_d)/2\\ T_1=\alpha T_2, T_2=1/(\sqrt{\alpha}\omega_d)\\ K=\left|K(j\omega_d)\right|/\left(\left|(1+T_1 s)/(1+T_2 s)\right|_{s=j\omega_d}\right)^2\end{cases} \tag{5}$$

IV. Case Studies

In order to demonstrate the POD performance using detailed HVDC models, the reduced 36-bus GB grid model is converted from DigSILENT/PowerFactory to RTDS. Detailed models of the VSC-HVDC links are used, as provided by the National HVDC Center [25]. For the case studies, a temporary three-phase line fault is applied in Zone 27W at t = 2s as the event trigger.

The adaptive POD performance is tested under three different system dispatches: default dispatch (Dispatch 1), low load/high renewable dispatch (Dispatch 2), and high load/low renewable dispatch (Dispatch 3). For the three dispatches, the optimal observation signal and actuator are selected in advance by using the method introduced in Section III. B. In this case study, the optimal observation signal is f_1-f_{32}, and the actuator is W.Coast 3 HVDC for P, Q, and P&Q modulation under three different dispatches. Therefore, the adaptive capability 1 in Figure 2 is not demonstrated in this case study.

The oscillation frequency and damping ratio of the dominant oscillation mode for the three dispatches are shown in TABLE I.

TABLE I. OSCILLATION MODE FOR DIFFERENT DISPATCH

Dispatch No.	Oscillation Freq. (Hz)	Damping Ratio (%)
1	0.89	3.11
2	0.85	0.82
3	0.77	5.07

According to Section III. C, the POD parameters are updated and listed in TABLE II. and TABLE III. for the three system dispatches. The active power modulation amplitude is usually limited within ±10% of the HVDC link's capacity. While the reactive power limit can be largely utilized for damping control, since the HVDC link only transmits the active power. Note that the parameters T_1 and T_2 are set to 0 to bypass the lead-lag blocks when using P modulation.

TABLE II. POD PARAMETERS FOR P MODULATION

Dispatch No.	T_w	ω_n	T_1/T_2	K	P limit (MW)
1	10	5.592	0/0	55	±400
2	10	5.341	0/0	220	±400
3	10	4.838	0/0	220	±400

TABLE III. POD PARAMETERS FOR Q MODULATION

Dispatch No.	T_w	ω_n	T_1/T_2	K	Q limit (MVar)
1	10	5.592	0.093/0.322	336.5	±1550
2	10	5.341	0.181/0.181	345.0	±1550
3	10	4.838	0.243/0.157	758.0	±1550

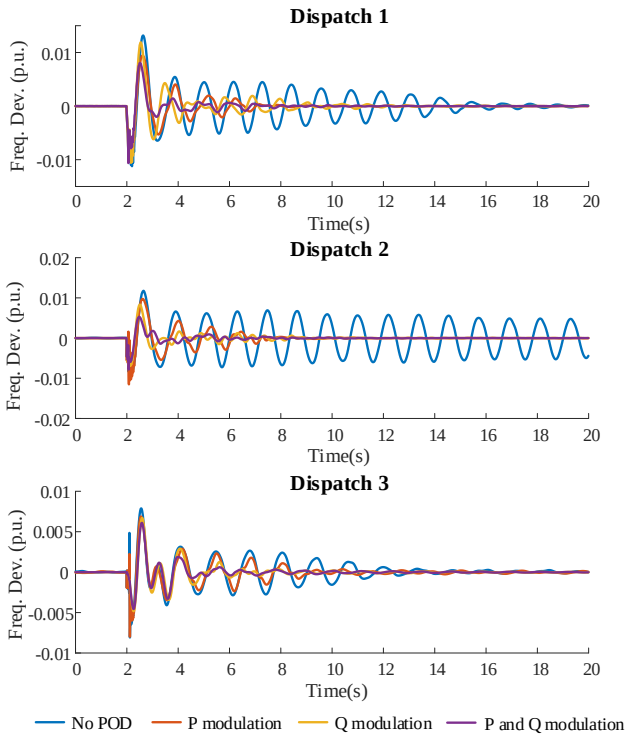

Figure 4. POD performance via P, Q, and P&Q modulation.

The POD control performances via P, Q, and P&Q modulation for Dispatch 1, 2 and 3 are given in Figure 4. From Figure 4, it can be proved that the designed POD controller can suppress the targeted oscillation mode via either P modulation or Q modulation for the three dispatches. The POD modulating both active and reactive power performs better than just modulating one of them.

To verify the necessity of the adaptive POD, the comparison of POD performance with non-adaptive and adaptive parameters under Dispatch 2 and 3 are shown in Figure 5 and Figure 6, respectively. Non-adaptive means the POD parameters designed for Dispatch 1 are used under Dispatch 2 or 3 (parameters in the first row of TABLE II and TABLE III). Adaptive refers to the specified parameters designed for Dispatch 2 or 3 (parameters in the second row for Dispatch 2 and third row for Dispatch 3). The oscillation frequency and damping ratio comparison are given in TABLE IV.

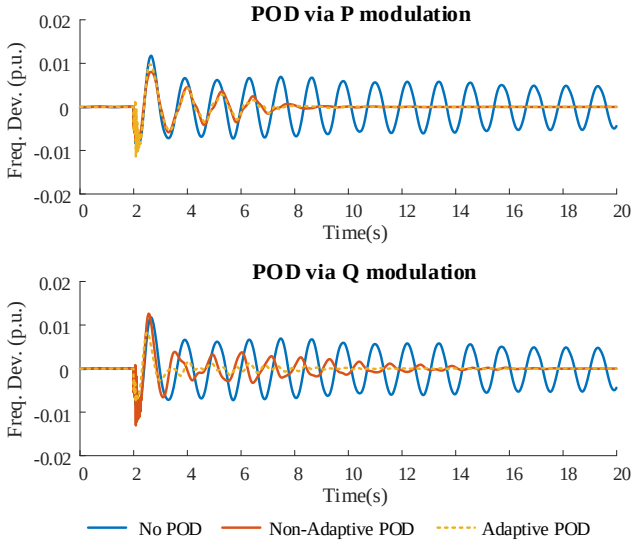

Figure 5. POD performance with different parameters under Dispatch 2.

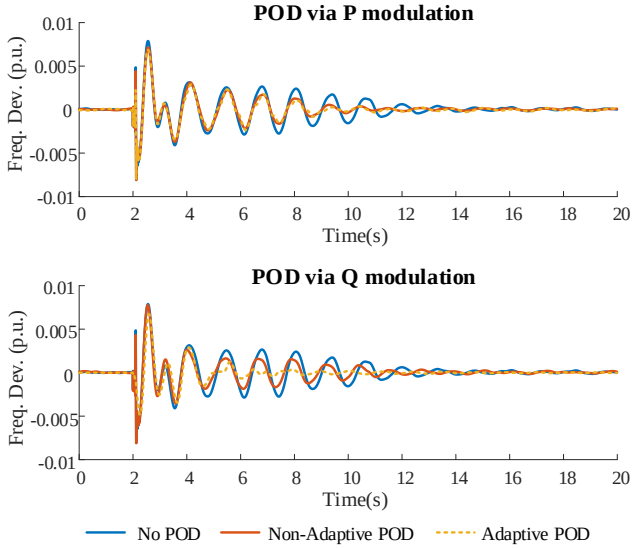

Figure 6. POD performance with different parameters under Dispatch 3.

With adaptive POD parameters, the damping performance can be improved for either P or Q modulation, especially via Q modulation. Compared to non-adaptive Q modulation, the damping ratio increases over 10% for Dipatch 2 and over 5% for Dispatch 3, which shows the effectiveness of the adapative POD design.

TABLE IV. ADAPTIVE POD PERFORMANCE

Dispatch No.	Scenario		Oscillation Freq. (Hz)	Damping Ratio (%)
2	No POD	N/A	0.85	0.82
	P modulation	Non-adaptive	0.83	11.32
		Adaptive	0.83	12.09
	Q modulation	Non-adaptive	0.92	**4.51**
		Adaptive	0.85	**>15**
3	No POD	N/A	0.77	5.07
	P modulation	Non-adaptive	0.75	7.48
		Adaptive	0.75	8.67
	Q modulation	Non-adaptive	0.77	**9.89**
		Adaptive	0.77	**>15**

V. CONCULUSION

In this paper, an adaptive wide-area POD controller via HVDC links is designed for the Great Britain power system. The POD input signal and the control parameters can be adjusted according to the various system operating conditions. Case studies using a GB model developed in RTDS demonstrate that: (1) The POD via either P, Q or P&Q modulation can damp the oscillation effectively; (2) The POD can effectively select the observation signal and actuator based on the system dispatch; (3) Under different system dispatches, the adaptive POD can adjust its control parameters. The damping effect shows that it performs better than the POD with fixed parameters, especially for POD via Q modulation.

REFERENCES

[1] Y. Yu, S. Grijalva, J. J. Thomas, L. Xiong, P. Ju and Y. Min, "Oscillation Energy Analysis of Inter-Area Low-Frequency Oscillations in Power Systems," *IEEE Trans. Power Syst.*, vol. 31, no. 2, pp. 1195-1203, March 2016.

[2] Y. Shu, X. Zhou and W. Li, "Analysis of low frequency oscillation and source location in power systems," *CSEE J. Power Energy Syst.*, vol. 4, no. 1, pp. 58-66, March 2018.

[3] Y. Hashmy, Z. Yu, D. Shi and Y. Weng, "Wide-Area Measurement System-Based Low Frequency Oscillation Damping Control Through Reinforcement Learning," *IEEE Trans. Smart Grid*, vol. 11, no. 6, pp. 5072-5083, Nov. 2020.

[4] H. A. Abumeteir and A. M. Vural, "Impact of High Penetration Renewable Energy Systems on Low-Frequency Oscillations," *2021 International Conference on Electric Power Engineering – Palestine* (ICEPE- P), 2021, pp. 1-4.

[5] A. U. Krismanto, M. Nadarajah and O. Krause, "Influence of renewable energy based microgrid on low frequency oscillation of power systems," *2015 IEEE PES Asia-Pacific Power and Energy Engineering Conference (APPEEC)*, 2015, pp. 1-5.

[6] L. Bo, L. Lin, L. Jun-Yong, L. You-Bo, Z. Wei and T. Jun-Jie, "An identification method for critical low frequency oscillation mode based on inter-area oscillation relevant generator contribution factor," *2014 International Conference on Power System Technology*, 2014, pp. 408-414.

[7] Y. Qiao, A. Xue, Z. Huang, T. Bi and C. Li, "Impact of close oscillation modes on the typical algorithms for the low frequency oscillation parameter identification of power systems," *2014 International Conference on Power System Technology*, 2014, pp. 655-661.

[8] Joe H. Chow, and Juan J. Sanchez-Gasca, "Power System Stabilizers," Power System Modeling, Computation, and Control, IEEE, 2020, pp.265-294.

[9] P. Arunagirinathan, Y. Wei, A. Arzani, and G. K. Venayagamoorthy, "Wide-Area Situational Awareness based Power System Stabilizer Tuning with Utility Scale PV Integration," *2018 Clemson University Power Systems Conference (PSC)*, 2018, pp. 1-8.

[10] Q. Zhong and G. Weiss, "Synchronverters: Inverters That Mimic Synchronous Generators," *IEEE Trans. Ind. Electron.*, vol. 58, no. 4, pp. 1259-1267, April 2011.

[11] L. Huang, H. Xin and Z. Wang, "Damping Low-Frequency Oscillations Through VSC-HVDC Stations Operated as Virtual Synchronous Machines," *IEEE Trans. Power Electron.*, vol. 34, no. 6, pp. 5803-5818, June 2019.

[12] X. Chen, W. Du, C. Chen and H. F. Wang, "Impact of strong dynamic couplings between VSC-based generation units and power systems on power system electro-mechanical oscillation modes," *2017 2nd International Conference on Power and Renewable Energy (ICPRE)*, 2017, pp. 93-97.

[13] V. Terzija, D. Cai and J. Fitch, "Monitoring of inter-area oscillations in power systems with renewable energy resources using Prony method," *CIRED 2009 - The 20th International Conference and Exhibition on Electricity Distribution* - Part 2, 2009, pp. 1-14.

[14] M. E. Aboul-Ela, A. A. Sallam, J. D. McCalley and A. A. Fouad, "Damping controller design for power system oscillations using global signals," *IEEE Trans. Power Syst.*, vol. 11, no. 2, pp. 767-773, May 1996.

[15] Y. A. I. Mohamed and E. F. El-Saadany, "Adaptive Decentralized Droop Controller to Preserve Power Sharing Stability of Paralleled Inverters in Distributed Generation Microgrids," *IEEE Trans. Power Electron.*, vol. 23, no. 6, pp. 2806-2816, Nov. 2008.

[16] X. Jin, J. Zhao, H. Wang, K. Li, L. Niu and H. Pan, "Design of Adaptive TCSC Damping Controller Based on Oscillation Energy Analysis," *2005 IEEE/PES Transmission & Distribution Conference & Exposition*: Asia and Pacific, 2005, pp. 1-5.

[17] S. V. Khatami, H. Soleymani and S. Afsharnia, "Adaptive neuro-fuzzy damping controller design for a power system installed with UPFC," 2010 Conference Proceedings IPEC, 2010, pp. 1046-1051.

[18] P. Korba, M. Larsson, B. Chaudhuri, B. Pal, R. Majumder, R. Sadikovic, G. Andersson, "Towards Real-time Implementation of Adaptive Damping Controllers for FACTS Devices," *2007 IEEE Power Engineering Society General Meeting*, 2007, pp. 1-6.

[19] S. Ranjbar, F. Haghjoo and M. R. Aghamohammadi, "Adaptive wide area damping controller for damping inter-area oscillations on power system," *2016 24th Iranian Conference on Electrical Engineering (ICEE)*, 2016, pp. 1609-1614.

[20] R. Preece, A. M. Almutairi, O. Marjanovic and J. V. Milanović, "Damping of inter-area oscillations using WAMS based supplementary controller installed at VSC based HVDC line," *2011 IEEE Trondheim PowerTech*, 2011, pp. 1-8.

[21] Ljung L. "System Identification: Theory for the User," Prentice Hall PTR, 1999.

[22] Y. Zhao, C. Lu, J. Yong, Y. Han, "Residue and identification based wide-area damping controller design in large-scale power system," *Proc. IEEE PES Conference on Innovative Smart Grid Technologies*, Washington. DC, USA, Jan. 2012.

[23] A. Heniche, and I. Kamwa. "Assessment of Two Methods to Select Wide-Area Signals for Power System Damping Control", *IEEE Trans. Power Syst.*, vol.23, pp. 572-581, May 2008.

[24] Y. Zhao, Z. Yuan, C. Lu, G. Zhang, X. L, and Y. Chen, "Improved model-free adaptive wide-area coordination damping controller for multiple-input–multiple-output power systems," *IET Gener. Transmiss. Distrib.*, vol. 13, pp. 3264-3275, Oct. 2016.

[25] D. Guo, M. H. Rahman, G. P. Ased, L. Xu, A. Emhemed, G. Burt, Y. Audichya. "Detailed quantitative comparison of half-bridge modular multilevel converter modelling methods." *The Journal of Engineering*, 2019, no. 16 (2019): 1292-1298.